Supplementary Information

Capturing the Multiscale Dynamics of Membrane Protein Complexes with All-Atom, Mixed-Resolution, and Coarse-Grained Models

Chenyi Liao,[†,1] Xiaochuan Zhao,[†,1] Jiyuan Liu,[†] Severin T. Schneebeli,[†] John C. Shelley,[‡] and Jianing Li[,†]*

[†]Department of Chemistry, The University of Vermont, Burlington, VT 05405

[‡]Schrödinger, Inc., 101 SW Main Street, Suite 1300, Portland, OR 97204

[1]Both authors contributed equally to this work.

Table of Contents

1. Modeling methods

1.1 Dimer model preparation

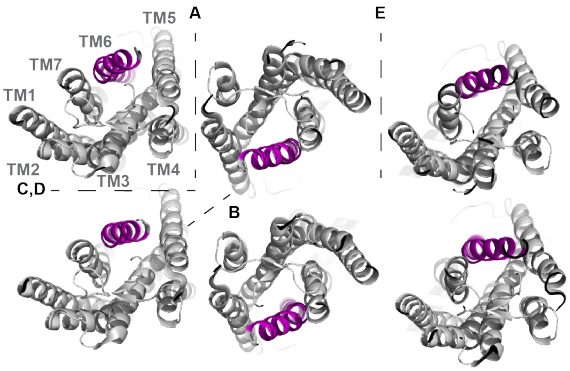

Fig. S1 Five heterodimeric interfaces used in our study from the rhodopsin cluster model (PDBID: 1N3M) in grey cartoon. Transmembrane helix 6 (TM6) is in magenta to guide the eyes. A2AR and D2R are switched in the C and D asymmetric complexes.

Table S1. Summary of the A2AR-D2R complex models.

Complex	D2R Model	Fit to 1N3M	Interface	A2AR Model	Fit to 1N3M	Interface
A	D2R-2	Chain A	TM4/5	A2AR*-1	Chain C	TM4/5
A’	D2R-2	Chain A	TM4/5	A2AR-2	Chain C	TM4/5
B	D2R-2	Chain A	TM4	A2AR*-1	Chain D	TM4
B’	D2R-2	Chain A	TM4	A2AR-2	Chain D	TM4
C	D2R-2	Chain A	TM1/2/3	A2AR*-1	Chain B	TM5/6
C’	D2R-2	Chain A	TM1/2/3	A2AR-2	Chain B	TM5/6
D	D2R-2	Chain B	TM5/6	A2AR*-1	Chain A	TM1/2/3
D’	D2R-2	Chain B	TM5/6	A2AR-2	Chain A	TM1/2/3
E	D2R-2	Chain D	TM1/H8	A2AR*-1	Chain F	TM1/H8
E’	D2R-2	Chain D	TM1/H8	A2AR-2	Chain F	TM1/H8

Note: For Models B and B’, the A2AR models were moved closer to the D2R models to form direct contacts, as in the D2R homodimer.[1] Each model has two simulation replicas.

1.2 Dimer models in complex with dual-acting ligands.

We built the dual-acting ligand models to distinguish models of different complexes. The binding of these ligands to the A2AR-D2R complexes has been proven by prior experiments.[2] The two moieties (ZM 2411385 and ropinirole) were connected by an alkane chain of seven or eleven carbon atoms (Fig. S2). The native distance between the ZM 2411385 center and the center of the A2A pocket is 2.4 Å (PDBID: 3EML). The native distance between the eticlopride molecule center and the center of the D3 pocket is 5.6 Å (PDBID: 3PBL). These values were used as reference distances of binding in our analysis. To build the ligand-bound complex models, the moieties were aligned to the ligand positions in the reference crystal structures, and the linkers were built to connect them in Maestro (Schrödinger, Inc.) Since ropinirole (pK_a value ~10) may be either protonated or deprotonated in our 40 different complex models, 80 ligand-bound complex models were constructed and simulated with the simulated annealing (SA) method in Desmond v3.

2. Simulated annealing simulations of A2AR-D2R complexes with dual-acting ligands.

A dual-acting ligand is believed to likely bind A2AR and D2R simultaneously, but on the molecular level the complex structures are not firmly established. To understand the binding mechanism of the dual-acting ligands and to assess the dimer models, we have built the models of the A2AR-D2R dimer complexed with the dual-acting compounds. In total, 80 complex models were constructed and simulated with the simulated annealing (SA) method. During each simulation, the temperature was increased from 10 K to 400 K in four stages over 600 ns, followed by 400 ns at 300 K (Table S2). The final models were evaluated with the centroid distances between the ligands and the GPCR binding sites, the percentage of residues that in native contacts with the GPCRs, and the distances between the centers of the ligands and the toggle switch Trp6.48 in both A2AR and D2R (Table S3).

Table S2. Five stages used for the simulated annealing simulations.

Stages	1	2	3	4	5
Duration (ps)	30	70	100	300	500
Temperature (K)	10	100	300	400	300

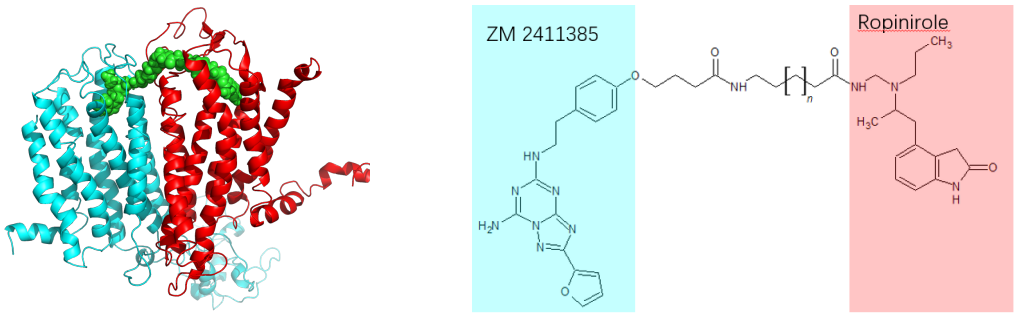

Fig. S2 Cartoon illustration of a stable ligand-bound model (complex A with the TM4/5-TM4/5 interface). *Left*: The ligand molecule is in the green sphere representation, while the GPCRs are in cartoon representations (A2AR in red and D2R in cyan). *Right*: The chemical structures of the dual-acting ligands. The ZM 2411385 and ropinirole moieties are highlighted with cyan and red backgrounds, where *n* is either 4 or 8 in the linker.

Table S3. Structural properties of the A2AR-D2R complex models bound to dual-acting ligands.

Complex	Centoid Distance[a] (Å)		Native Contact Percentage[b] (%)		RMSD (Å)		Distance between $Trp^{6.48}$ & Ligand Centroid[c] (Å)	
	A2AR	D2R	A2AR	D2R	A2AR	D2R	A2AR	D2R

A	3.4	4.2	72	63	2.5	2.5	12.4	11.8
A[d]	7.7	7.8	55	45	3.0	2.6	16.6	12.3
B	12.4	13	46	49	3.4	2.8	15.0	16.2
B[d]	15.4	10.6	37	45	3.1	2.9	18.9	13.8
C	7.4	11.0	47	35	3.3	3.6	14.4	11.8
C[d]	4.5	10.9	69	25	2.8	4.1	12.2	11.7
D	11.3	7.4	43	24	2.6	3.1	5.1	6.9
D[d]	3.9	11.6	78	11	2.3	2.5	10.5	12.9
E	11.3	10.2	48	28	3.1	2.3	14.4	11.2
E[d]	9.3	9.5	69	37	3.0	2.3	14.3	10.8

[a] The distance between the A2AR or D2R pocket center and the corresponding binding ligand center. The reference distances from the crystal structures are 2.4 and 5.6 Å respectively.

[b] The number of residues in A2AR or D2R in contact with the ligand after SA simulations compared to the reference structure.

[c] The distance between the C_α atom of $Trp^{6.48}$ in A2AR or D2R and the corresponding ligand center**.** The reference distances from the crystal structures are 11.0 and 8.0 Å respectively.

[d] Protonated ligands.

Our results provide evidence that the dual-acting ligands are capable of forming tight complexes with the A2AR-D2R dimer, interacting with both GPCR ligand-binding sites. However, given the constraints of the linker, the complexes with the TM4/5-TM4/5 interface (Fig. S2) seem to be more favorable for dual-acting ligand binding. The others with larger separations between A2AR and D2R are less favorable for simultaneous binding of the dual-acting ligands.

Our data also suggest that the protonation state of the ligand and the linker length may have an impact on dual-acting ligand binding. The ligands with longer linkers bind the GPCR heterodimer models more tightly, while ligands with shorter linkers tend to bind to either A2AR or D2R. Overall, we only observed that the ligands stay tightly bound to the complex A model, which emphasizes the importance of the TM4/5-TM4/5 interface.

3. Supplementary analysis for Table 1.

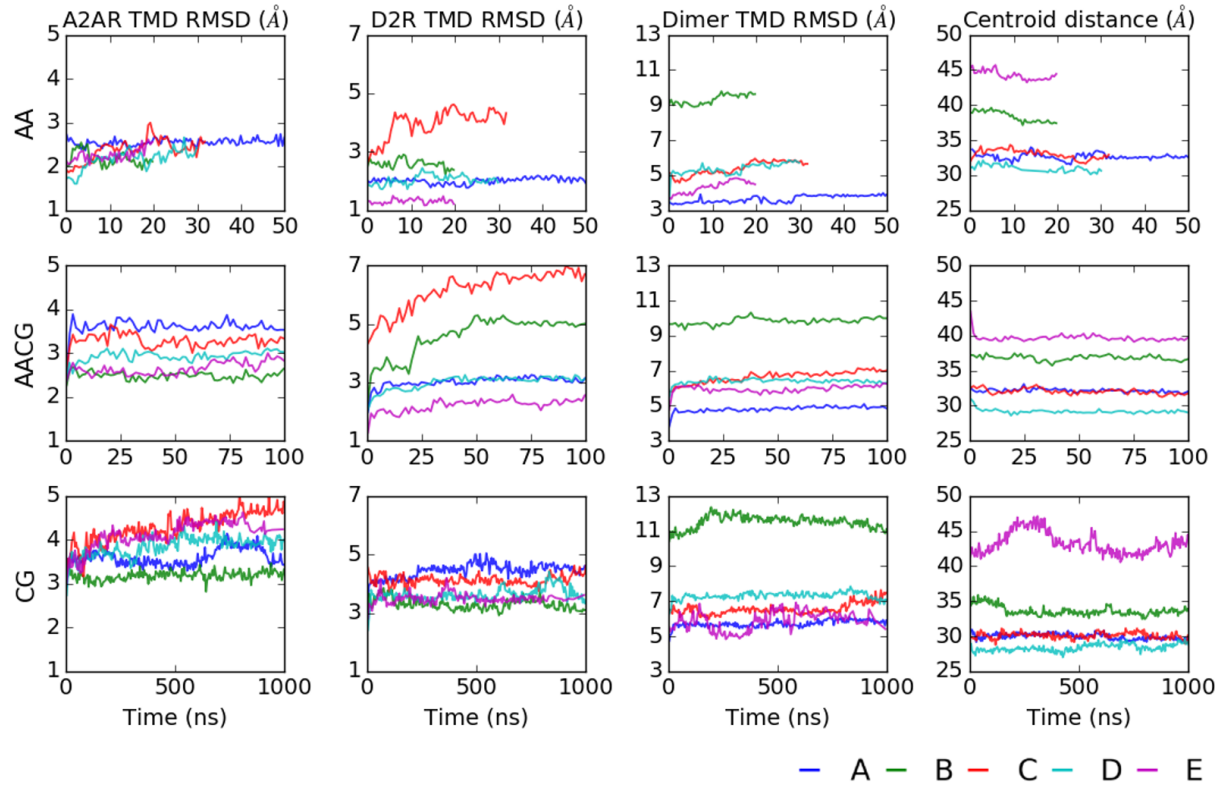

Fig. S3 Time evolutions of TMD RMSDs and centroid distances. Each plot was generated from one representative run.

Table S4. Distance ranges of the A2AR C-tail (represented by C_α of res. 325) and the D2R ICL3 (represented by C_α of res. 222) in different complex models.

Complex	D_{AA} (Å)	D_{AACG} (Å)	D_{CG} (Å)	Effective range[3] of FRET and BRET (Å)
A	50-70	45-70	50-70	10~60
B	60-70	55-70	50-70	
C	90-100	85-110	80-90	
D	60-70	60-70	50-60	
E	15-25	15-25	15-25	

4. Brief description of the AACG potentials.

4.1 AACG parameterization. The AACG potentials cover the standard and modified amino acids, the backbone capping groups, Na^+ and Cl^- ions, the POPC lipid, and the cosolvents (i.e. isopropanol,

isopropylamonium, acetamide, and acetate). The AACG energy function resembles the one of the OPLS force field,[4] which has the bonded and non-bonded terms. (1) Most of the parameters for the bonded terms remained the same as in the OPLS force field for the proteins/peptides, while some small adjustments were made for the torsions. (2) The non-bonded terms involving the CG region adopted a polynomial form, but the pair-wise Coulombic and 12-6 Lennard-Jones potentials were retained for the AA region. While the detailed parameterization process was described in another publication[5], an overall description is provided herein: with a number of long AA simulations as references, the initial AACG potentials were generated with the force-matching method[5]. Further improvement was carried out by identifying the cause of distortions in the protein structures and adding incremental changes to the potentials. Within the CG region and between the AA and CG regions, several hundred cycles of adjustment were made, as automated by local computer programs.

4.2 AACG validation. The development of the AACG model was based upon many AA simulations of pure POPC membranes, globular proteins, a transmembrane protein, and small peptides. We have tested and validated the potentials with a number of integral membrane proteins (like class A and class B GPCRs) in the POPC bilayer and peptides (*i.e.* melittin, chignolin, and Trp-cage) in water. The self-assembly of 20 melittin molecules was simulated, which demonstrated good agreements with prior experimental results and our AA simulations.[5] These results show evidence to support the effectiveness and transferability of the AACG potentials.

5. Examination of the AA models recovered from the CG models.

We performed the recovery from the CG to the AA models, in order to examine the model stability. In the AA simulations with the recovered models, we observed structurally stable dimer models as shown by the C_α RMSDs in the transmembrane domains (Fig. S4).

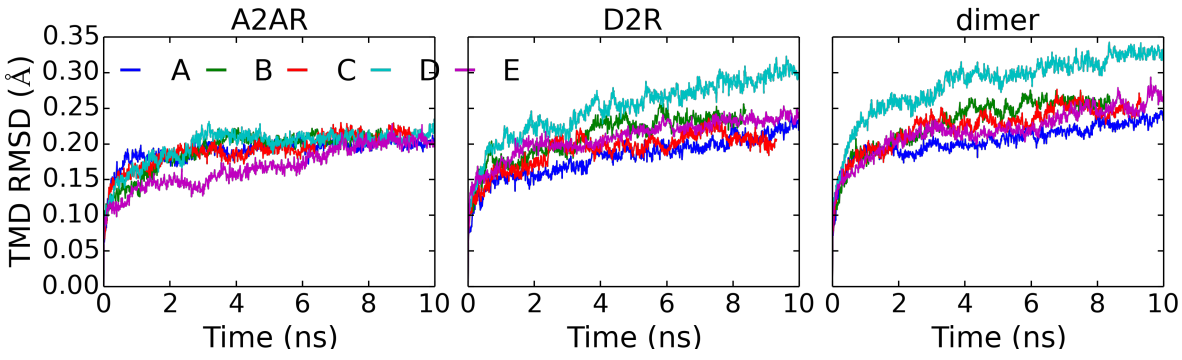

Fig. S4 Time evolutions of the TMD C_α RMSDs for individual A2AR/D2R and the entire dimer complexes using the AA models recovered from the MARTINI CG models.

References:

(1) Guo, W.; Shi, L.; Filizola, M.; Weinstein, H.; Javitch, J. A. Crosstalk in G protein-coupled receptors: Changes at the transmembrane homodimer interface determine activation. *Proc. Natl. Acad. Sci. U. S. A.* **2005,** *102* (48), 17495-17500.

(2) Joerg, M.; May, L. T.; Mak, F. S.; Lee, K. C. K.; Miller, N. D.; Scammells, P. J.; Capuano, B. Synthesis and Pharmacological Evaluation of Dual Acting Ligands Targeting the Adenosine A(2A) and Dopamine D-2 Receptors for the Potential Treatment of Parkinson's Disease. *J. Med. Chem.* **2015,** *58* (2), 718-738.

(3) Fuxe, K.; Ferre, S.; Canals, M.; Torvinen, M.; Terasmaa, A.; Marcellino, D.; Goldberg, S. R.; Staines, W.; Jacobsen, K. X.; Lluis, C.; Woods, A. S.; Agnati, L. F.; Franco, R. Adenosine A2A and dopamine D2 heteromeric receptor complexes and their function. *J. Mol. Neurosci.* **2005,** *26* (2-3), 209-20.

(4) Jorgensen, W. L.; Maxwell, D. S.; Tirado-Rives, J. Development and Testing of the OPLS All-Atom Force Field on Conformational Energetics and Properties of Organic Liquids. *J. Am. Chem. Soc.* **1996,** *118*, 11225-11236.

(5) Shelley, M. Y.; Selvan, M. E.; Zhao, J.; Babin, V.; Liao, C.; Li, J.; Shelley, J. C. A new mixed all-atom/coarse-grained model: application to melittin aggregation in aqueous solution. *J. Chem. Theory Comput.* **Under Review**.